Legged Robot Estimation - A Decoupled Approach via Moving Horizon Estimation and Invariant Filters

Jiarong Kang and Xiaobin Xiong University of Wisconsin-Madison

Abstract—In this abstract, we present a modular state estimation framework for legged robots that decouples floating-base orientation estimation—handled via an invariant EKF—from the estimation of physical quantities such as contact forces and inertial parameters using a Moving Horizon Estimation (MHE) approach. This design leverages system symmetries and naturally incorporates robot dynamics and deterministic constraints. Building on prior hardware validation, we further integrate recent advances in differential dynamics and numerical optimization to model contact interactions within the estimation process.

Project Repositories: [State_MHE], [Force_State_MHE].

I. Introduction

Legged robot state estimation typically focuses on recovering the floating base states using a relatively compact set of onboard sensors. Recent advances in exploiting symmetry properties have improved the accuracy of both proprioceptiveonly estimators [1] [2] and those incorporating exteroceptive sensors [3], enabling robust pose estimation across a range of operational scenarios. Unlike wheeled or aerial platforms, legged robots are commonly modeled with hybrid dynamics in control applications due to the discrete nature of foot-ground interactions. In contrast, the differences in state estimation across platforms often stem more from the types and configurations of available sensors than from fundamental differences in system dynamics. While traditional estimators have primarily focused on pose estimation, recent work has extended legged robot state estimation to include contact/disturbance force [4] and even inertial parameter identification [5] by leveraging contact-rich dynamics.

Despite these advances, effectively incorporating complex, and potentially hybrid, dynamics into real-time estimation frameworks remains a significant challenge. This motivates further investigation into structured estimators—such as those based on invariant filtering/smoothing or moving horizon estimation (MHE)—that can better exploit the physical and geometric structure of legged locomotion systems.

However, the symmetry structure of legged robots under hybrid dynamics remains insufficiently understood. To address this, we adopt a decoupled approach [6], [7]: the floating-base state is estimated using a well-established invariant EKF [8], while a Moving Horizon Estimation (MHE)-based optimization framework flexibly estimates physical quantities such as contact forces. This modular design improves adaptability and has been shown to naturally incorporate robot dynamics and deterministic constraints in previous work. Building on this foundation, recent advances in differential contact dynamics

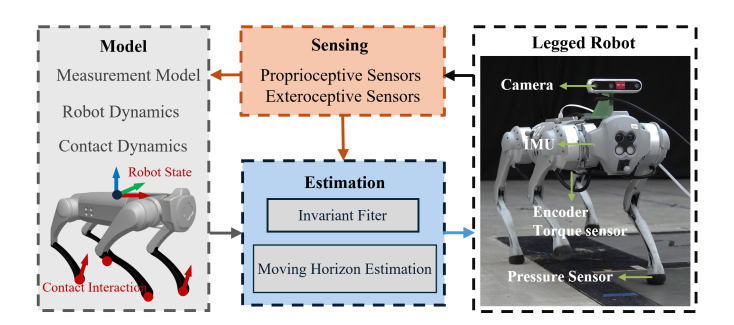


Fig. 1. Illustration of the proposed decoupled estimation framework applied to various legged robots. Experimental results are also available in [6] and [7].

[9] and numerical optimization [10] further enable seamless integration of contact dynamics into the framework.

In this abstract, we present three formulations of the proposed optimization-based estimator: (i) floating base state-only estimation [6], (ii) simultaneous estimation of state and ground reaction forces [7], both from prior work, and (iii) preliminary results of a unified estimator that jointly recovers state, contact interactions, and parameters of physical models.

II. BACKGROUND

A. Symmetry-Aware Estimation

Symmetry-Aware Estimation—specifically, invariant estimation methods—leverages the Lie group structure of robotic systems to enhance robustness and consistency. The Invariant Extended Kalman Filter (InEKF) exploits the group-affine property to construct autonomous error dynamics that are independent of the current state estimate, resulting in more accurate linearization [1]. Similarly, invariant smoothers use group-affine residuals with state-independent Jacobians, providing improved numerical conditioning and faster convergence within a history-preserving smoothing framework [11]. These characteristics make invariant estimator especially well-suited for contact-rich, highly dynamic environments [2], [8].

B. Optimization-based Estimation

Moving Horizon Estimation (MHE) and factor graph-based methods are both classical smoothing approaches that optimize over a sliding window of sensor data. Factor graphs, originating from the SLAM domain, typically assume a fixed structure and have been widely used to tightly fuse vision, IMU, and encoder measurements through preintegration [12]. However, its relatively fixed structure limits their flexibility in handling complex constraints or integrating with advanced numerical

optimization techniques, such as shooting methods [10], [13]. Moreover, little research has been conducted on leveraging system symmetries within the factor graph framework.

In contrast, MHE offers a more flexible optimization framework. As the dual of Model Predictive Control (MPC), MHE naturally incorporates robot dynamics and physical constraints, making it particularly well-suited for legged robots with contact-rich dynamics [14]. Unlike factor graphs, MHE can directly encode hybrid dynamics and contact constraints, providing improved consistency and constraint handling. Recent advances in computational techniques from the control domain [10] [15] may also advance the computation of MHE.

III. CONTACT INVOLVED ESTIMATION

This work aims to estimate both the robot state and its contact interactions with the environment. By leveraging robot and Linear Complementarity Problem based contact dynamics, along with onboard proprioceptive and exteroceptive measurements, we estimate the robot state and contact interactions without relying on high-fidelity force/torque sensing [6] [7].

A. Dynamics Modeling

1) Lagrangian Dynamics Modeling in Continuous Domain: The configuration of a legged robot is typically represented as $\mathbf{x} = \begin{bmatrix} \mathbf{q}^\mathsf{T} & \mathbf{v}^\mathsf{T} \end{bmatrix}^\mathsf{T}$, where $\mathbf{q} \in SE(3) \times \mathbb{R}^n$ denotes the generalized coordinates, including the floating-base pose \mathbf{p} and \mathbf{R} , and the joint positions α , with n representing the number of actuated joints. The generalized velocity is given by $\mathbf{v} \in \mathfrak{se}(3) \times \mathbb{R}^n$, comprising both the base twist and joint velocities. Under the assumption of known and static contact interactions, the holonomic constrained Lagrangian dynamics of the rigid body system in continuous time can be expressed as:

$$\mathbf{M}(\mathbf{q})\dot{\mathbf{v}} + \mathbf{h}(\mathbf{q}, \mathbf{v}) = \mathbf{B}\mathbf{u} + \sum_{i} \mathbf{J}_{i}(\mathbf{q})^{\top} \mathbf{f}_{i},$$
 (1)

$$\mathbf{J}_i(\mathbf{q})\dot{\mathbf{v}} + \mathbf{J}(\dot{\mathbf{q}})\mathbf{v} = \mathbf{0},\tag{2}$$

where the term $\mathbf{M}(\mathbf{q}) \in \mathbb{R}^{(6+n)\times(6+n)}$ represent the inertia matrix, and $\mathbf{h}(\mathbf{q},\mathbf{v})$ is the bias vector including Coriolis, centrifugal and gravitational effects. The input matrix $\mathbf{B} \in \mathbb{R}^{(6+n)\times n}$ maps the joint torque vector \mathbf{u} to the generalized force space. The term $\mathbf{f}_i \in \mathbb{R}^3$ represents the contact force or ground reaction force (GRF) at the i-th contact point, and $\mathbf{J}_i(\mathbf{q}) \in \mathbb{R}^{3\times(6+n)}$ is the associated contact Jacobian.

2) Contact Dynamics Modeling via LCP: For rigid body systems modeled by Lagrangian dynamics, the continuous-time dynamics can be approximated by a discrete-time system using a semi-implicit Euler integration scheme:

$$\mathbf{q}^{+} - \mathbf{q} = \Delta t \, \mathbf{v}^{+},$$

$$\mathbf{M}(\mathbf{q})(\dot{\mathbf{v}}^{+} - \dot{\mathbf{v}}) = \Delta t (\mathbf{B}\mathbf{u} - \mathbf{h}(\mathbf{q}, \mathbf{v}) + \sum_{i} \mathbf{J}_{i}(\mathbf{q})^{\mathsf{T}} \mathbf{f}_{i}),$$
(3)

where Δt denotes the discrete time interval used for integration. Instead of enforcing holonomic constraints—since the contact mode is not known a priori—the contact impulse $\Delta t \, \mathbf{f}_i$ is computed using a time-stepping formulation of the Linear Complementarity Problem (LCP) based on a rigid contact model and polyhedral approximated friction cone [16].

Non-penetration: For contact at the next time step $(\cdot)^+$, both the signed distance between two bodies $\phi(\mathbf{q}^+)$ and the normal contact force f^n during the interval must be non-negative. Moreover, normal contact forces can only be nonzero when two bodies are in contact: $\phi(\mathbf{q}^+) \geq 0 \perp f^n \geq 0$. A linear approximation of this condition is used for computation:

$$\phi(\mathbf{q}) + \nabla \phi(\mathbf{q})(\mathbf{q}^+ - \mathbf{q}) \ge 0 \perp f^n \ge 0. \tag{4}$$

Maximum Dissipation: The maximum dissipation principle assumes that tangential friction forces act to maximize the dissipation of kinetic energy. For clarity, the formulation is presented for a single contact scenario:

$$\min_{\mathbf{A}} \quad \mathbf{f}_i^{\mathsf{T}} \mathbf{J}_i(\mathbf{q}) \dot{\mathbf{v}}^+ \tag{5}$$

s.t.
$$\mathbf{f} = \mathbf{n}f^n + \mathbf{D}\boldsymbol{\beta}, \ \boldsymbol{\beta} \ge \mathbf{0},$$
 (6)

$$\mu f^n - \mathbf{e}^\mathsf{T} \boldsymbol{\beta} \ge 0. \tag{7}$$

The Coulomb friction model is approximated using a polyhedral cone, where $\bf n$ is the unit normal vector at the contact point, and $\bf D$ positively span the tangential contact plane with unit vectors. The vector $\boldsymbol{\beta}$ represents the friction force coefficients along the directions defined by $\bf D$, μ is the coefficient of friction, and $\bf e$ is a vector of ones.

The Karush–Kuhn–Tucker (KKT) conditions of the resulting minimization problem, when combined with the discrete-time robot dynamics (3) and the non-penetration condition (4), define the contact dynamics as:

$$\mathbf{x}^{+} = \mathbf{LCP}(\mathbf{x}, \mathbf{u}). \tag{8}$$

The LCP-based contact dynamics admit analytical gradients, which can be leveraged to accelerate numerical performance in optimization based algorithm [9].

B. Measurement Modeling

1) IMU Model: In general, a discrete time single rigid body (SRB) dynamics model is used to model the IMU:

$$\begin{bmatrix} \mathbf{p}^{+} \\ \dot{\mathbf{p}}^{+} \\ \mathbf{R}^{+} \\ \mathbf{b}^{+}_{a} \\ \mathbf{b}^{+}_{\omega} \end{bmatrix} = \begin{bmatrix} \mathbf{p} + \Delta t \dot{\mathbf{p}} + \frac{1}{2} \Delta t^{2} \left(\mathbf{R} (\tilde{\mathbf{a}} - \mathbf{b}_{a}) + \mathbf{g} \right) \\ \dot{\mathbf{p}} + \Delta t \left(\mathbf{R} (\tilde{\mathbf{a}} - \mathbf{b}_{a}) + \mathbf{g} \right) \\ \mathbf{R} \operatorname{Exp} \left(\Delta t (\tilde{\omega} - \mathbf{b}_{\omega})^{\times} \right) \\ \mathbf{b}_{a} \\ \mathbf{b}_{\omega} \end{bmatrix} \oplus \boldsymbol{\delta}_{\text{IMU}}, (9)$$

where \mathbf{p} , \mathbf{R} , \mathbf{b}_a , and \mathbf{b}_ω denote the floating-base (or IMU) position, orientation, accelerometer bias, and gyroscope bias, respectively. The operator $\text{Exp}(\cdot)$ denotes the matrix exponential, and $(\cdot)^{\times}$ represents the skew-symmetric matrix associated with the given vector. \oplus is the additive operator on manifold. δ denotes the associated Gaussian noise.

2) Encoder and Kinematics Model: The legged robot is equipped with joint encoders that measure joint angles α and angular velocities $\dot{\alpha}$, both corrupted by Gaussian noise:

$$\tilde{\alpha} = \alpha + \delta_{\alpha}, \quad \dot{\tilde{\alpha}} = \dot{\alpha} + \delta_{\dot{\alpha}}.$$
 (10)

Given known leg kinematics, the foot's relative position and velocity in the body frame can be expressed as:

$$\mathbf{R}^{\mathsf{T}}(\mathbf{p}_{\text{foot}} - \mathbf{p}) = \mathbf{f}\mathbf{k}_{\mathcal{B}}(\tilde{\alpha}) + \boldsymbol{\delta}_{\text{pf}},\tag{11}$$

$$\mathbf{R}^{\mathsf{T}}(\dot{\mathbf{p}}_{\text{foot}} - \dot{\mathbf{p}}) = \mathbf{J}_{\mathcal{B}}(\tilde{\alpha})\dot{\tilde{\alpha}} + (\tilde{\omega} - \mathbf{b}_{\omega})^{\times} \mathbf{f} \mathbf{k}_{\mathcal{B}}(\tilde{\alpha}) + \boldsymbol{\delta}_{\text{vf}}, \quad (12)$$

where $\mathbf{fk}_{\mathcal{B}}(\cdot)$ and $\mathbf{J}_{\mathcal{B}}(\cdot)$ are the foot's forward kinematics and Jacobian, respectively in body frame \mathcal{B} . The noise terms capture uncertainties from encoder noise, IMU noise, calibration, and model inaccuracies [17].

3) Visual Odometry Model: Visual Odometry (VO) measures the robot pose in the camera frame $\mathcal C$ by tracking features in the images from onboard cameras. Without loop closure [18], the VO output is interpreted as the incremental homogeneous transformation between consecutive camera frames $\mathcal C_i$ and $\mathcal C_j$: $\mathbf T_{\mathcal C ij} = \mathbf T_{\mathcal W \mathcal C_i}^{-1} \mathbf T_{\mathcal W \mathcal C_j} \oplus \delta_{\text{VO}}$, where $\mathbf T_{\mathcal W \mathcal C_i}$ and $\mathbf T_{\mathcal W \mathcal C_j}$ are the homogeneous transformations from the world frame $\mathcal W$ to the camera frame $\mathcal C$ at time i and j. The VO measurement is corrupted by noise δ_{VO} . With known fixed transformation $\mathbf T_{\mathcal B \mathcal C}$ between IMU/body frame $\mathcal B$ and camera frame $\mathcal C$, the body frame transformation $\mathbf T_{\mathcal B_{ij}}$ is used as measurements:

$$\tilde{\mathbf{T}}_{\mathcal{B}_{ij}} = \mathbf{T}_{\mathcal{B}\mathcal{C}} \tilde{\mathbf{T}}_{\mathcal{C}_{ij}} \mathbf{T}_{\mathcal{B}\mathcal{C}}^{-1}.$$
 (13)

C. Invariant EFK for Floating-base Estimation

The InEKF exploits the symmetry of a system represented by a matrix Lie group. Based on the IMU/SRB model, the IMU states without additive bias are embedded in the extended special Euclidean group with additional spatial vectors, denoted as $SE_2(3)$ [8]:

$$\mathbf{X} := \begin{bmatrix} \mathbf{R} & \dot{\mathbf{p}} & \mathbf{p} \\ \mathbf{0}^{1 \times 3} & 1 & 0 \\ \mathbf{0}^{1 \times 3} & 0 & 1 \end{bmatrix}. \tag{14}$$

In the absence of additive bias, the IMU state dynamics are group-affine. The right-invariant error, defined as η ,

$$\boldsymbol{\eta} = \hat{\mathbf{X}}\mathbf{X}^{-1} = \begin{bmatrix} \hat{\mathbf{R}}\mathbf{R}^{\top} & \hat{\mathbf{p}} - \hat{\mathbf{R}}\mathbf{R}^{\top}\hat{\mathbf{p}} & \hat{\mathbf{p}} - \hat{\mathbf{R}}\mathbf{R}^{\top}\mathbf{p} \\ \mathbf{0}_{1\times3} & 1 & 0 \\ \mathbf{0}_{1\times3} & 0 & 1 \end{bmatrix}, (15)$$

evolves according to an autonomous system. The log-linear property of this error propagation enables the formulation of the standard Invariant Extended Kalman Filter (InEKF) [1]. For legged robots with IMU bias and kinematic measurements, [8] extends the standard InEKF and demonstrates prominent performance. In this work, we adopt the InEKF developed in [8], with an additional velocity correction based on leg kinematics, to provide lightweight orientation estimation.

D. Real-time Optimization-based Estimation

Moving Horizon Estimation (MHE) is formulated as an optimization problem that minimizes the negative log-likelihood of the Maximum A Posteriori (MAP) estimate over a receding time window [19], as illustrated in Fig. 2. The optimization

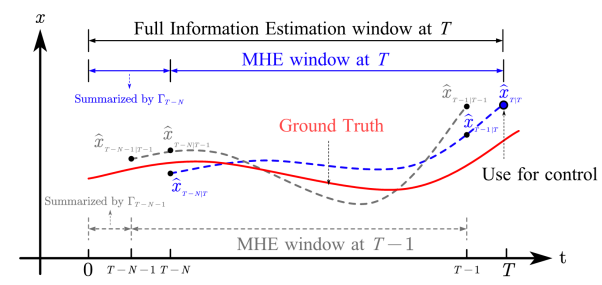


Fig. 2. Illustration of MHE, arrival cost Γ and their relationship with Full Information Estimation, where $\hat{x}_{i|k}$, $\{i,k\in\mathbb{N}^+|\ 0\le i\le k\le T\}$ is the estimate at time index i, using measurements from time 0 to time k.

incorporates both the system dynamics (Section II.A) and measurement models (Section II.B):

$$\min_{\mathbf{x}, \boldsymbol{\delta}_{[T-N,T]}} \Gamma(\mathbf{x}_{T-N})
+ \sum_{k=0}^{T-1} ||\boldsymbol{\delta}_k^{\mathbf{x}}||_{\text{Cov}_{\mathbf{x}}^{-1}}^2 + \sum_{k=0}^{T} ||\boldsymbol{\delta}_k^{\mathbf{y}}||_{\text{Cov}_{\mathbf{y}}^{-1}}^2$$
(MHE)

s.t.
$$\mathbf{x}_{k+1} = \mathbf{Dyn}(\mathbf{x}_k, \mathbf{u}_k) \oplus \boldsymbol{\delta}_k^{\mathbf{x}}, \ \forall k \in \{T - N, ..., T - 1\}$$

 $\mathbf{y}_k = \mathbf{Meas}(\mathbf{x}_k) \oplus \boldsymbol{\delta}_k^{\mathbf{y}}, \ \forall k \in \{T - N, ..., T\},$
 $\mathbf{0} \leq \mathbf{Constr}(\mathbf{x}_k), \ \forall k \in \{T - N, ..., T\}.$

The arrival cost term $\Gamma(\cdot)$ is computed using an Extended Kalman Filter or derived following the procedure outlined in our previous work [6]. To meet real-time requirements that exceed the control frequency, we either exploit invariant properties through decentralization or leverage differential structure to enable fast numerical computation.

- 1) Decentralized MHE as Quadratic Program: In our prior work [6], the decentralized MHE framework uses a standalone InEKF for accurate and well-converged orientation estimation. This decentralization enables the dynamics and measurement models in Sections III.A and III.B to be reformulated as linear constraints within the MHE, which is subsequently cast as a convex Quadratic Program (QP). To further construct a convex optimization problem that accounts for the robot dynamics in (1) and contact dynamics in (8), the estimation of contact mode and joint states is also decoupled using direct measurements results from pressure sensors and joint encoders [7].
- 2) Nonlinear MHE through Differential Dynamic Programming: By leveraging the differential properties of the robot dynamics (1) or the contact dynamics (8), the nonlinear optimization problem (MHE) can be efficiently solved using Differential Dynamic Programming (DDP), even in the presence of complementarity constraints introduced by contact dynamics. By analyzing the Bellman equation of (MHE), the value function can be recursively expressed as:

$$V(\mathbf{x}) = \min_{\delta} Q(\mathbf{x}, \delta), \tag{16}$$

$$Q(\mathbf{x}, \boldsymbol{\delta}) = V^{+}(\mathbf{x}^{+}) + L(\mathbf{x}, \boldsymbol{\delta}), \tag{17}$$

where $V(\mathbf{x})$ is the value function, and $Q(\mathbf{x}, \boldsymbol{\delta})$ is the unoptimized value function. In DDP, the model uncertainty $\boldsymbol{\delta}$ is computed to minimize the local second-order approximation

of Q at the current estimated trajectory $(\hat{\cdot})$:

$$Q(\mathbf{x}, \boldsymbol{\delta}) \approx Q(\hat{\mathbf{x}}, \hat{\boldsymbol{\delta}}) + \Delta Q,$$
 (18)

$$\Delta Q = \frac{1}{2} \begin{bmatrix} 1\\ \delta \mathbf{x} \\ \delta \boldsymbol{\delta} \end{bmatrix}^{\mathsf{T}} \begin{bmatrix} 0 & \nabla_{\mathbf{x}} Q^{\mathsf{T}} & \nabla_{\boldsymbol{\delta}} Q^{\mathsf{T}} \\ \nabla_{\mathbf{x}} Q & \nabla_{\mathbf{x}}^{\mathsf{T}} Q & \nabla_{\mathbf{x}\boldsymbol{\delta}} Q \\ \nabla_{\boldsymbol{\delta}} Q & \nabla_{\boldsymbol{\delta}\mathbf{x}} Q & \nabla_{\boldsymbol{\delta}}^{\mathsf{T}} Q \end{bmatrix} \begin{bmatrix} 1\\ \delta \mathbf{x} \\ \delta \boldsymbol{\delta} \end{bmatrix} . \tag{19}$$

Minimizing ΔQ w.r.t. $\delta \delta$ yields the optimal uncertainty:

$$\delta \delta^* = \mathbf{K} \cdot \delta \mathbf{x} + \alpha \mathbf{k},\tag{20}$$

$$\mathbf{K} = -\nabla_{\boldsymbol{\delta}}^2 Q^{-1} \nabla_{\boldsymbol{\delta} \mathbf{x}} Q, \quad \mathbf{k} = -\nabla_{\boldsymbol{\delta}}^2 Q^{-1} \nabla_{\boldsymbol{\delta}} Q.$$

When applying DDP to state estimation, the initial state is assumed to follow a prior distribution $\Gamma(\cdot)$, as indicated in (MHE). During DDP, the optimal perturbation to the initial state $\delta \mathbf{x}_0$ is generally non-zero and is computed as:

$$\delta \mathbf{x}_0^* = -\left[\nabla_{\mathbf{x}_0}^2 V\right]^{-1} \nabla_{\mathbf{x}_0} V. \tag{21}$$

IV. EVALUATION

A. Prior Results

In our previous work, we evaluated the proposed estimation framework on the commercial quadrupedal robot Unitree Go1 in two scenarios: (i) robot state-only estimation [6] and (ii) simultaneous estimation of robot state and ground reaction forces [7]. To address the computational challenges of the canonical optimization-based estimator (MHE), we adopted a decentralized structure as described in Section III.D.1), leveraging system symmetry by decoupling orientation estimation using a standalone InEKF, as detailed in Section III.C.

The estimator is implemented in C++ within ROS2 environment. The MHE is solved using OSQP [20], and VO is provided by the open-source ORB-SLAM3 [18]. The InEKF is adapted from the open-source implementation in [8]. The MHE runs at 200 Hz. The complete software implementation for both scenarios is publicly available at [21], [22].

Robot State Estimation: For robot state estimation, our method outperforms the EKF [23] and InEKF [8] baselines that fuse IMU and leg odometry as indicated in Table. I. We further evaluate MHE estimation accuracy and computation time in Fig. 3 by varying the window size from 1 to 20. The RMSE improves with larger windows due to the inclusion of more VO frames, highlighting the benefit of MHE in leveraging windowed measurements for precise state estimation.

TABLE I
RMSEs of the state estimations on Go1 hardware.

RINGES OF THE STATE ESTIMATIONS ON GOT HARDWARE.							
Estimation	Our Method	Our Method	EFK	InEKF			
Method		(w/o VO)					
RMSE _p [m/s]	0.0654	0.0847	0.0901	0.0817			
RMSE _{Euler} [rad]	0.0160	0.0230	0.0218	0.0157			

 $TABLE \ II \\ RMSEs \ of \ the \ state \ and \ force \ estimations \ on \ Go1 \ hardware.$

Estimation Method	Our Method	Our Method (w/o Phys.)	DKF	MBO
RMSE _p [m/s]	0.0504	0.0497	0.0628	NA
RMSE _f [N]	6.6790	11.2255	10.1594	12.7229

Robot State and GRF Estimation: For robot state and GRF estimation, we use the same onboard sensing configuration

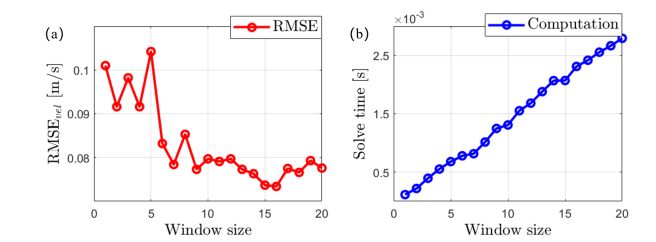


Fig. 3. Window size effects. (a) Accuracy improves w.r.t. window size. (b) Computational cost increases approximately linearly w.r.t. window size.

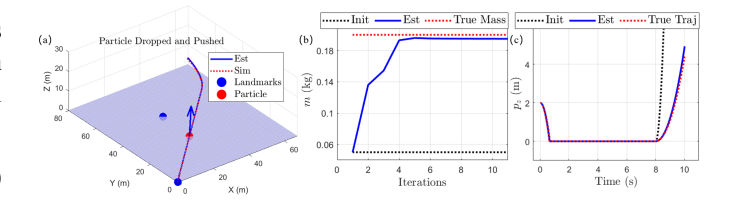


Fig. 4. (a) Particle experiment illustration; (b) Inertial parameter estimation result; (c) State estimation result. The estimated inertial parameters converge to the ground truth, and the state trajectory also aligns with the true trajectory with updated contact mode.

as in the robot state estimation task. As shown in Table II, compared to baseline momentum-based methods [4] [24], exteroceptive sensors enhance estimation accuracy, while contact constraints further enforce physical consistency.

B. Preliminary Results

Robot State, Contact Model and Physical Parameter Estimation: For robot state, contact mode and parameter estimation, contact dynamics are incorporated into the MHE framework. All physical constraints are embedded within the LCP formulation, resulting in a dynamics-constrained windowed optimization problem solvable via DDP. The simulation and estimation are implemented in MATLAB, with the DDP implementation adapted from [25]. Leveraging its differential structure and smoothed analytical gradients [26], the proposed method successfully recovers the trajectory, contact mode, and inertial parameters in a scenario where a particle is dropped and pushed on a frictional surface. As illustrated in Fig. 4, the particle mass is estimated from biased initial guesses, with corresponding refinements in contact mode and state.

V. FUTURE WORK AND DISCUSSION

In this work, we presented a Moving Horizon Estimation (MHE) framework that incorporates robot and contact dynamics. System symmetry is addressed through decoupled orientation estimation using a standalone InEKF. Building on existing hardware and simulation results, our ongoing efforts aim to evaluate the proposed contact-aware MHE on real hardware with real-time implementation. Future directions include incorporating invariant cost terms into the MHE to further enhance estimation consistency [2], and more deeply exploiting the symmetry inherent in legged robot dynamics. We also aim to extend this framework to contact-rich scenarios in robot manipulation [27] and aerial robotic manipulation [28].

REFERENCES

- [1] A. Barrau and S. Bonnabel, "The invariant extended kalman filter as a stable observer," *IEEE Transactions on Automatic Control*, vol. 62, no. 4, pp. 1797–1812, 2017.
- [2] Z. Yoon, J.-H. Kim, and H.-W. Park, "Invariant smoother for legged robot state estimation with dynamic contact event information," *IEEE Transactions on Robotics*, vol. 40, pp. 193–212, 2024.
- [3] Y. Nisticò, H. Kim, J. C. V. Soares, G. Fink, H.-W. Park, and C. Semini, "Multi-sensor fusion for quadruped robot state estimation using invariant filtering and smoothing," *IEEE Robotics and Automation Letters*, vol. 10, no. 6, pp. 6296–6303, 2025.
- [4] J. Kang, H. Kim, and K.-S. Kim, "View: Visual-inertial external wrench estimator for legged robot," *IEEE Robotics and Automation Letters*, vol. 8, no. 12, pp. 8366–8373, 2023.
- [5] S. Martinez, R. J. Griffin, and C. Mastalli, "Multi-contact inertial parameters estimation and localization in legged robots," 2025. [Online]. Available: https://arxiv.org/abs/2403.17161
- [6] J. Kang, Y. Wang, and X. Xiong, "Fast decentralized state estimation for legged robot locomotion via ekf and mhe," *IEEE Robotics and Automation Letters*, vol. 9, no. 12, pp. 10914–10921, 2024.
- [7] J. Kang and X. Xiong, "Simultaneous ground reaction force and state estimation via constrained moving horizon estimation," in 2025 IEEE International Conference on Robotics and Automation (ICRA), 2025.
- [8] R. Hartley, M. Ghaffari, R. M. Eustice, and J. W. Grizzle, "Contactaided invariant extended kalman filtering for robot state estimation," *The International Journal of Robotics Research*, vol. 39, no. 4, pp. 402–430, 2020
- [9] G. Kim, D. Kang, J.-H. Kim, and H.-W. Park, "Contact-implicit differential dynamic programming for model predictive control with relaxed complementarity constraints," in 2022 IEEE/RSJ International Conference on Intelligent Robots and Systems (IROS). IEEE, 2022, pp. 11978–11985.
- [10] C. Mastalli, R. Budhiraja, W. Merkt, G. Saurel, B. Hammoud, M. Naveau, J. Carpentier, L. Righetti, S. Vijayakumar, and N. Mansard, "Crocoddyl: An efficient and versatile framework for multi-contact optimal control," in 2020 IEEE International Conference on Robotics and Automation (ICRA). IEEE, 2020, pp. 2536–2542.
- [11] P. Chauchat, A. Barrau, and S. Bonnabel, "Invariant smoothing on lie groups," in 2018 IEEE/RSJ International Conference on Intelligent Robots and Systems (IROS), 2018, pp. 1703–1710.
- [12] S. Yang, Z. Zhang, Z. Fu, and Z. Manchester, "Cerberus: Low-drift visual-inertial-leg odometry for agile locomotion," in 2023 IEEE International Conference on Robotics and Automation (ICRA). IEEE, 2023, pp. 4193–4199.
- [13] F. Farshidian et al., "OCS2: An open source library for optimal control of switched systems," [Online]. Available: https://github.com/ leggedrobotics/ocs2.

- [14] X. Xinjilefu, S. Feng, and C. G. Atkeson, "Dynamic state estimation using quadratic programming," in 2014 IEEE/RSJ International Conference on Intelligent Robots and Systems. IEEE, 2014, pp. 989–994.
- [15] A. Aydinoglu, A. Wei, W.-C. Huang, and M. Posa, "Consensus complementarity control for multi-contact mpc," *IEEE Transactions on Robotics*, 2024.
- [16] P. Varin and S. Kuindersma, "A constrained kalman filter for rigid body systems with frictional contact," in Algorithmic Foundations of Robotics XIII: Proceedings of the 13th Workshop on the Algorithmic Foundations of Robotics 13. Springer, 2020, pp. 474–490.
- [17] S. Teng, M. W. Mueller, and K. Sreenath, "Legged robot state estimation in slippery environments using invariant extended kalman filter with velocity update," 2021 IEEE International Conference on Robotics and Automation (ICRA), pp. 3104–3110.
- [18] C. Campos, R. Elvira, J. J. G. Rodriguez, J. M. M. Montiel, and J. D. Tardos, "Orb-slam3: An accurate open-source library for visual, visual-inertial, and multimap slam," *IEEE Transactions on Robotics*, vol. 37, no. 6, p. 1874–1890, Dec. 2021.
- [19] C. Rao, J. Rawlings, and D. Mayne, "Constrained state estimation for nonlinear discrete-time systems: stability and moving horizon approximations," *IEEE Transactions on Automatic Control*, vol. 48, no. 2, pp. 246–258, 2003.
- [20] B. Stellato, G. Banjac, P. Goulart, A. Bemporad, and S. Boyd, "OSQP: an operator splitting solver for quadratic programs," *Mathematical Programming Computation*, vol. 12, no. 4, pp. 637–672, 2020.
- [21] github.com/well-robotics/Decentralized_EKF_MHE.
- [22] github.com/well-robotics/Force_State_Estimation.
- [23] M. Blösch, M. Hutter, M. A. Höpflinger, S. Leutenegger, C. Gehring, C. D. Remy, and R. Y. Siegwart, "State estimation for legged robots consistent fusion of leg kinematics and imu," in *Robotics: Science and Systems*. 2012.
- [24] J. Hu and R. Xiong, "Contact force estimation for robot manipulator using semiparametric model and disturbance kalman filter," *IEEE Trans*actions on Industrial Electronics, vol. 65, no. 4, pp. 3365–3375, 2018.
- [25] M. Kobilarov, D.-N. Ta, and F. Dellaert, "Differential dynamic programming for optimal estimation," in 2015 IEEE International Conference on Robotics and Automation (ICRA), 2015, pp. 863–869.
- [26] G. Kim, D. Kang, J.-H. Kim, S. Hong, and H.-W. Park, "Contact-implicit model predictive control: Controlling diverse quadruped motions without pre-planned contact modes or trajectories," *The International Journal of Robotics Research*, vol. 44, no. 3, pp. 486–510, 2025.
- [27] T. Pang, H. T. Suh, L. Yang, and R. Tedrake, "Global planning for contact-rich manipulation via local smoothing of quasi-dynamic contact models," *IEEE Transactions on robotics*, vol. 39, no. 6, pp. 4691–4711, 2022.
- [28] J. Welde, J. Paulos, and V. Kumar, "Dynamically feasible task space planning for underactuated aerial manipulators," *IEEE Robotics and Automation Letters*, vol. 6, no. 2, pp. 3232–3239, 2021.